Vorticity Model of Flow Driven by Purely Poloidal Currents

P. M. Bellan
California Institute of Technology, Pasadena, California 91125
(Received 15 June 1992)

The axisymmetric, incompressible, viscoresistive magnetohydrodynamic equations for purely poloidal currents $I(r,z)$ are transformed into three coupled *scalar* partial differential equations. These show that finite $\partial I/\partial z$ acts as a *volumetric source of fluid "vorticity"* which drives strong poloidal flows (jets).

PACS numbers: 52.80.Mg, 52.55.Ez, 52.75.Di, 98.60.Qs

Axisymmetric, purely poloidal current configurations are found in a wide variety of conducting fluids and plasmas. Terrestrial examples include electric furnace [1] and other industrial arcs [2], magnetoplasma-dynamic (MPD) thrusters [3], z pinches [4], Marshall guns [5], thyratrons [6], ignitrons, lightning, liquid metals [7], and electrolytes. Although astrophysical plasmas are typically assumed to have both toroidal and poloidal currents, there presumably exist situations where the current is primarily poloidal (Refs. [8,9] are possible examples).

The most interesting property of these configurations, a strong axial acceleration of fluid or plasma away from regions of constricted current, was first discussed by Maecker [10]. Axially directed fluid velocities of the order of the Alfvén velocity can result from this acceleration, and in a high current arc most [11] of the electrical energy input can go into translational kinetic energy, rather than into thermal energy or radiation. The thrust associated with this axial flow is the basis of the MPD rocket engine, while in electric arc furnaces, viscous dissipation of the arc kinetic energy heats the metal being processed. Arc axial flow velocities have been measured by Bowman [12] and by Irie and Barrault [13]. Reed [14] graphically demonstrated the flow in liquid mercury. Numerical magnetohydrodynamic (MHD) models for electric arc furnaces have been discussed by McKelliget and Szekely [15] and for MPD thrusters by La Pointe [16].

We present here a new interpretation of this phenomenon which shows that *axial current inhomogeneity* acts as a *volumetric source of fluid "vorticity."* Our model assumes an incompressible, constant density fluid; this is reasonable for liquids but is an oversimplification for gases (compressibility considerations will alter the *response* to the vorticity generation mechanism discussed here, but should not affect the mechanism itself).

The relevant equations are the MHD equation of motion

$$\rho[\partial\mathbf{U}/\partial t+\mathbf{U}\cdot\nabla\mathbf{U}]=\mathbf{J}\times\mathbf{B}-\nabla P+\rho\nu\nabla^2\mathbf{U}\,, \tag{1}$$

where ρ and ν are, respectively, the mass density and kinematic viscosity; the MHD Ohm's law

$$\mathbf{E}+\mathbf{U}\times\mathbf{B}=\eta\mathbf{J}\,; \tag{2}$$

and Ampere's and Faraday's laws

$$\nabla\times\mathbf{B}=\mu_0\mathbf{J},\quad \nabla\times\mathbf{E}=-\partial\mathbf{B}/\partial t\,. \tag{3}$$

The electric field is $\mathbf{E}=-\nabla\Phi-\partial\mathbf{A}/\partial t$ and we choose the Coulomb gauge $\nabla\cdot\mathbf{A}=0$, i.e., $\mathbf{A}=\nabla f\times\nabla\theta$, where f is a scalar function and we use cylindrical coordinates (r,θ,z) so that $\nabla\theta=\hat{\boldsymbol{\theta}}/r$.

Since the θ component of Eq. (1),

$$\rho\left[\frac{\partial(rU_\theta)}{\partial t}+\mathbf{U}\cdot\nabla(rU_\theta)\right]=\rho\nu\left[r\frac{\partial}{\partial r}\frac{1}{r}\frac{\partial}{\partial r}(rU_\theta)+\frac{\partial^2}{\partial z^2}(rU_\theta)\right], \tag{4}$$

contains no driving force term, finite U_θ is possible only in the exceptional situations where (i) it has been imposed as an initial condition at the initial time t_0 (after which U_θ transiently decays), or (ii) it is imposed as a boundary condition on some external bounding surface. Situation (i) implies that the assumption of axisymmetry and purely poloidal currents was violated before t_0 while (ii) implies that the assumption is violated at some point in space external to the bounding surface. We assume here that neither of these exceptional situations occurs, in which case $U_\theta=0$.

The most general poloidal velocity for a constant density, incompressible fluid has the form

$$\mathbf{U}=(2\pi)^{-1}\nabla\psi\times\nabla\theta\,, \tag{5}$$

where $\psi(r,z)$ is the fluid flux (streamline) function. For this cylindrical geometry problem, it is useful to define the "vorticity" $\chi\equiv r\hat{\boldsymbol{\theta}}\cdot\nabla\times\mathbf{U}$ so that

$$\nabla\times\mathbf{U}=\chi\nabla\theta\,; \tag{6}$$

note that χ differs by a factor of r from the usual definition of vorticity. Equations (5) and (6) give the cylindrical version of the well-known result that vorticity acts as a source term in a Poisson-like equation for ψ,

$$r^2\nabla\cdot(r^{-2}\nabla\psi)=-2\pi\chi\,. \tag{7}$$

Because of axisymmetry, Ampere's law gives the current density and magnetic field to be, respectively,

$$\mathbf{J}=(2\pi)^{-1}\nabla I\times\nabla\theta,\quad \mathbf{B}=\mu_0(2\pi)^{-1}I\nabla\theta\,, \tag{8}$$

where $I(r,z)$ is the total current linked by a circle of radius r with center at z. Comparison of Eqs. (5) and (8) shows that I acts as the streamline for $\mathbf{J}$.

We now assume there is a constriction of characteristic radius r_c in the current channel (e.g., for a z-pinch

sausage instability, r_c would be the sausage "neck" radius, while for an arc r_c would be the cathode radius); this constriction implies the current is axially nonuniform, i.e., $\partial I/\partial z \neq 0$. We change to dimensionless (tilde) variables by normalizing all lengths to r_c, magnetic fields to the field $B_c = \mu_0 I_c/2\pi r_c$, and velocities to the Alfvén velocity $V_{Ac} = B_c/(\mu_0\rho)^{1/2}$ (here subscript c means evaluated at $r = r_c$ on the current constriction). Thus, one obtains

$$\begin{aligned} r &= r_c\tilde{r}, \quad z = r_c\tilde{z}, \quad t = (r_c/V_{Ac})\tilde{t}, \\ \psi &= V_{Ac}r_c^2\tilde{\psi}, \quad \chi = V_{Ac}\tilde{\chi}, \quad I = I_c\tilde{I}, \\ U &= V_{Ac}\tilde{U}, \quad \mathbf{B} = B_c\tilde{I}\tilde{\nabla}\theta, \quad A = B_c r_c\tilde{A}, \\ P &= (B_c^2/\mu_0)\tilde{P}, \quad \Phi = V_{Ac}B_c r_c\tilde{\Phi}. \end{aligned} \tag{9}$$

Dropping the tildes, the dimensionless equation of motion becomes

$$\nabla\left(\frac{U^2}{2}+P+\frac{I^2}{2r^2}\right)+\left[\nabla\left(\frac{1}{2\pi}\frac{\partial\psi}{\partial t}\right)-\chi\mathbf{U}-\hat{\mathbf{z}}\frac{I^2}{r^2}+\frac{1}{R}\nabla\chi\right]\times\nabla\theta=0, \tag{10}$$

where

$$R = r_c V_{Ac}/\nu = \mu_0^{1/2} I_c/2\pi\nu\rho^{1/2} \tag{11}$$

is the hydrodynamic Reynolds number. Similarly Ohm's law becomes

$$-\nabla\Phi-\partial\mathbf{A}/\partial t+\mathbf{U}\times I\nabla\theta = S^{-1}\nabla I\times\nabla\theta, \tag{12}$$

where

$$S = r_c V_{Ac}\mu_0/\eta = \mu_0^{3/2} I_c/2\pi\eta\rho^{1/2} \tag{13}$$

is the magnetic Reynolds number (or Lundquist number, since the characteristic velocity is V_{Ac}). Equations (10) and (12) are of the form

$$\nabla g+\mathbf{Q}\times\nabla\theta=0, \tag{14}$$

which is the most general form of an axisymmetric partial differential equation (PDE) involving a potential. We can extract *two* scalar PDE's from Eq. (14) by (i) operating with $\nabla\theta\cdot\nabla\times$ and (ii) taking the divergence. Doing the former we see that Eq. (14) becomes $\nabla\cdot(r^{-2}\mathbf{Q})=0$, which using Eqs. (10) and (7) gives

$$\frac{\partial}{\partial t}\left(\frac{\chi}{r^2}\right)+\nabla\cdot\left(\frac{\chi}{r^2}\mathbf{U}\right)=\nabla\cdot\left(\frac{1}{Rr^2}\nabla\chi\right)-\frac{1}{r^4}\frac{\partial I^2}{\partial z}. \tag{15}$$

The left-hand side of Eq. (15) shows that the modified vorticity quantity χ/r^2 is convected with the fluid. The right-hand side shows that viscosity acts as a dissipative-diffusive term for the vorticity, and most importantly that $r^{-4}\partial I^2/\partial z$ acts as a *volumetric source* of vorticity. This is in contrast to ordinary fluid mechanics where typically there are no volumetric sources of vorticity, and instead vorticity is generated by viscous drag at surfaces producing torques on the fluid. Because of the r^{-4} coefficient we see that the vorticity source is concentrated at small r. For a uniform current density extending up to a radius r_c (e.g., the cathode for an arc), $r^{-4}I^2$ is uniform in r for $r < r_c$ and then falls off as r^{-4} for $r > r_c$. Similarly the z dependence will be strongest near the cathode and so we conclude that the vorticity source is strongly localized to be just above the face of the cathode.

Thus, we can imagine the term $r^{-4}\partial I^2/\partial z$ acts like a set of paddlewheels located just above or below the constriction; these impart torques to the fluid which start circulations having on-axis flows away from the constriction. The fluid velocity field [second term on the left-hand side of Eq. (15)] convects vorticity away from the source, so that a plume of vorticity develops and follows the fluid streamlines. The vorticity plume is ultimately dissipated by viscosity so that eventually the flow becomes irrotational.

Likewise, operating on Eq. (12) with $\nabla\theta\cdot\nabla\times$ gives

$$\frac{\partial}{\partial t}\left(\frac{I}{r^2}\right)+\nabla\cdot\left(\frac{I}{r^2}\mathbf{U}\right)=\nabla\cdot\left(\frac{1}{Sr^2}\nabla I\right). \tag{16}$$

Aside from missing a source term, this induction equation appears formally identical to Eq. (15). The lack of a source term in Eq. (16) indicates that the conversion of current into vorticity cannot be run in reverse, i.e., an axial nonuniformity in χ does not drive a current. The absence of dynamo action is consistent with Cowling's [17] antidynamo theorem that axisymmetric flows cannot drive steady currents. Besides the lack of a source term in Eq. (16), Eqs. (15) and (16) also differ in that $\mathbf{U}$ is a function of ψ which is a function of χ, i.e., $\mathbf{U}=\mathbf{U}(\psi(\chi))$, which gives the usual fluid convective nonlinearity in Eq. (15). In contrast, for Eq. (16) we have to extend the chain of dependence one step further, and consider $\mathbf{U}=\mathbf{U}(\psi(\chi(I)))$. Thus, more complicated types of nonlinearities could appear in Eq. (16) at high S.

We see that in the limit $S\to\infty$, the quantity I/r^2 convects with (is frozen into) the fluid. That this is the same as the familiar concept that magnetic flux is frozen into the fluid can be seen by considering a thin toroidal ring-shaped element of fluid with major radius r and minor cross-section area σ. Since the fluid is incompressible, the ring volume $2\pi r\sigma$ stays constant as the ring convects and distorts; thus $\sigma\sim r^{-1}$. The toroidal magnetic flux in the ring is $B_\theta\sigma\sim I/r^2$ and so, using Eq. (16), is frozen into the ring when $S\to\infty$. Similarly, for large R and no vorticity source, Eq. (15) becomes the Kelvin circulation theorem for this geometry, since the fluid circulation around the minor cross section of the ring is $\oint\mathbf{U}\cdot d\mathbf{l}=(\nabla\times\mathbf{U})_\theta\sigma\sim\chi/r^2$.

Additional insight regarding Eq. (16) for large S can be gained by considering the vector $\mathbf{T}\equiv\nabla(I/r^2)\times\nabla\theta$, which peaks at the outer edge of the current distribution. For large S and in steady state, Eq. (16) gives $\mathbf{U}\cdot\nabla(I/r^2)\approx 0$, which is equivalent to $\mathbf{U}\times\mathbf{T}\approx 0$. Thus,

for large S, Eq. (16) shows that the edge of the current distribution tends to line up with the velocity field, whereas for small S the current distribution diffuses across the velocity field.

Equations (7), (15), and (16) provide a complete system of equations for the three scalar functions ψ, χ, and I; all that is required are temporal initial conditions and spatial boundary conditions to define a specific problem.

Let us now consider pressure and electric potential, which did not appear in Eqs. (7), (15), and (16) since these quantities only appeared in the g-type term of Eq. (14). We can obtain equations for P and Φ by taking the divergence of the analogs of Eq. (14) in which case we obtain equations of the form

$$\nabla^2 g = -\nabla\theta\cdot\nabla\times\mathbf{Q} \tag{17}$$

with Neumann boundary conditions specified by Eq. (14). Since $\mathbf{Q}$ depends only on ψ, χ, and I, which were obtained from the solutions of the coupled Eqs. (7), (15), and (16), we see that in Eq. (17), the right-hand side can simply be considered as a known source term for a Poisson's equation. Equation (17) can be simplified, by integrating it over the volume of a square minor cross-section "torus," in which case it becomes

$$\int d\mathbf{S}\cdot\nabla g = -2\pi\oint d\mathbf{l}\cdot\mathbf{Q}\,, \tag{18}$$

where the line integral is the short (poloidal) way around the torus. Thus, the respective equations for pressure and potential are

$$\int d\mathbf{S}\cdot\nabla P^* = 2\pi\oint \mathbf{dl}\cdot(\chi\mathbf{U} - R^{-1}\nabla\chi + \hat{\mathbf{z}}r^{-2}I^2)\,, \tag{19}$$

where $P^* = P + U^2/2 + I^2/2r^2$, and

$$\int d\mathbf{S}\cdot\nabla\Phi = 2\pi\oint d\mathbf{l}\cdot(I\mathbf{U} - S^{-1}\nabla I)\,. \tag{20}$$

Equations (7), (15), (16), (19), and (20) have been numerically integrated for parameters relevant to a steady-state high current arc using simultaneous overrelaxation (SOR) on a 40×40 grid with upwind differencing and a flux-preserving cylindrical differencing scheme. Additionally, a spectral method (Fourier transform in z) was used to solve the time-dependent Eqs. (7), (15), and (16). Total arc current was 50 kA, cathode current density was 4×10^7 A/m^2, $n=10^{23}$ m^{-3}, amu $=50$, $\eta=10^{-4}\Omega$ m, and $\nu=0.01\eta/\mu_0$. These parameters give $r_c=2\times10^{-2}$ m, $B_c=0.5$ T, $V_{Ac}=4.89\times10^3$ m/sec, $S=1.24$, and $R=124$. For simplicity, spatially uniform η and ν were used; spatial dependence (e.g., due to temperature dependence) would result in R and S becoming nonuniform, giving more realistic (i.e., sharper) arc boundaries than obtained here. Boundary conditions were chosen to be no-slip ($\mathbf{U}=0$) on the top (located at $z=10r_c$) and bottom ($z=0$) surfaces, and $U_r=0$ at $r=0$. The boundary conditions on the right-hand surface (i.e., at $r=10r_c$) were specified by assuming that the streamlines were horizontal on this surface, i.e., $U_z=0$ and also $\partial U_z/\partial r=0$. The condition $U_z=0$ on the right-hand side gives the Neumann condition on ψ that $\partial\psi/\partial r=0$, while the condition $\partial U_z/\partial r=0$ inserted into Eq. (7) gives the Dirichlet condition on χ that $\chi_{\rm rhs}=-(2\pi)^{-1}[\partial^2\psi/\partial z^2]_{\rm rhs}$. The evolution of the simpler SOR method qualitatively followed the time-dependent result, namely, χ/r^2 was first generated above the cathode and then convected, plumelike, with the flow along the fluid streamlines until a steady state was obtained. Figure 1 shows the steady-state SOR solution for χ/r^2 (shaded contours), with velocity vectors superimposed; note the plume of χ/r^2 which emanates from just above the cathode, and convects with the fluid streamlines. Figure 2 shows the corresponding solution for P (shaded contours), with the current streamlines shown as solid lines.

Along the line $r=0$ (symmetry axis), regularity requires $I=0$, $\chi=0$, $\partial P^*/\partial r=0$. Thus, *along this axis* Eq.

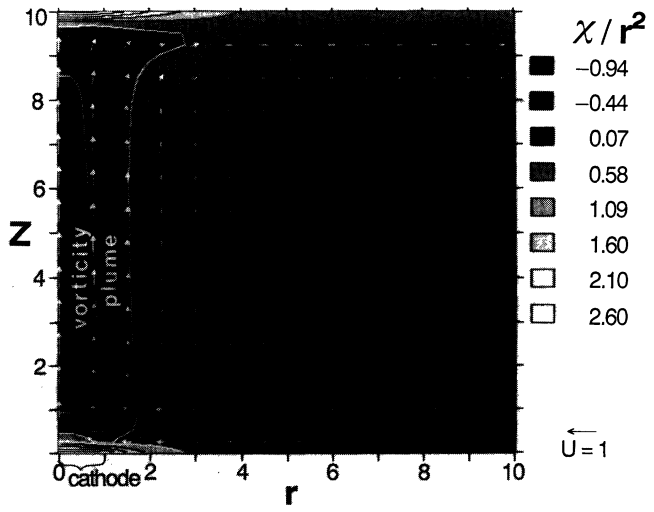

FIG. 1. χ/r^2 (shaded contours) and velocity vectors.

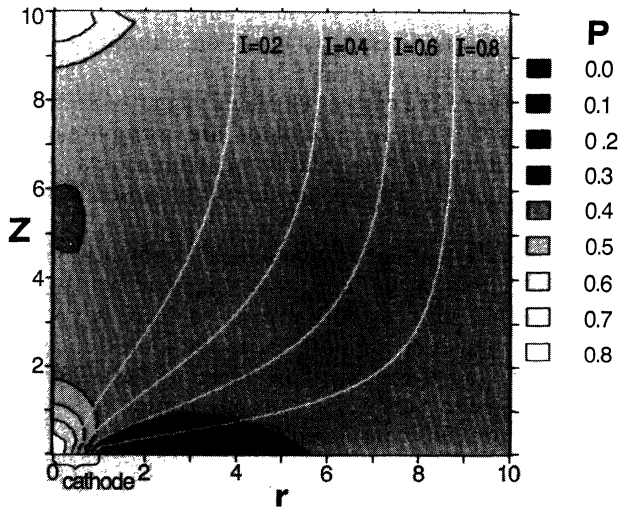

FIG. 2. P (shaded contours) and current streamlines.

(19) becomes the Bernoulli relation $P+U^2/2 \approx$ const; cf. Fig. 1. The situation is more complicated on the line $z=0$ where there is an interplay between Bernoulli effects, viscous drag, and magnetic confining forces. Equation (19) shows that on the line $z=0$, the viscous drag term $R^{-1}\partial\chi/\partial z$ depresses the pressure when $\partial\chi/\partial z$ is negative. Because the vorticity plume is a depression in χ [cf. Fig. 1], $\partial\chi/\partial z$ is negative for $z=0^+$, $r<1$, causing the peak pressure to be *significantly below* the Bennett pinch [18] value of unity. Furthermore, the no-slip boundary condition (i.e., $U_r=0$) associated with the material surface at $z=0$ causes a boundary layer of reverse (i.e., positive) vorticity just above $z=0$ (and also at just below $z=10$), where the tangential fluid velocity abruptly drops to zero. This also gives negative $\partial\chi/\partial z$ on the line $z=0$ producing further pressure depression extending to radii beyond the plume. For a z pinch or astrophysical jet where $z=0$ is simply a line of symmetry (i.e., no material surface) and so finite U_r is allowed, there is no reverse vorticity boundary layer and so only the plume-induced pressure depression occurs.

This viscous drag-induced pressure depression below the Bennett value is consistent with the unexpected observation in a high current arc experiment by Jones *et al.* [19] that the peak pressure at $r=0$ on the cathode was about half the Bennett value. [Jones *et al.* postulated that the observed pressure reduction was caused by outward centrifugal force due to "swirl" (i.e., finite U_θ) partially canceling the inward pinch pressure, but did not present direct experimental evidence from their arc supporting this postulate.]

For the vorticity plume to be important, the axial extent of the problem must reasonably exceed r_c so that the plume has room to develop; similarly, R should be reasonably large so that the plume has a chance to travel some distance before it is dissipated by viscosity. For large R velocities of the order of V_{Ac} are attained.

A consequence of this acceleration of plasma away from a current constriction is that a z pinch [4] undergoing a sausage instability will have fluid jets expelling plasma axially from the constricted region. Also, many astrophysical phenomena involve poloidal currents [20] and constrictions of the current channels ought to produce jets here as well. Likely candidates are astrophysical jets [21], which have strong axial flows and pinchlike confinement [8], and the solar polar current proposed by Alfvén [20].

The purely toroidal magnetic-field configurations considered in this paper have *zero* magnetic helicity [22]. Poloidal flux surfaces do not exist so there is no Grad-Shafranov equation (in contrast to the finite helicity, axisymmetric, nondissipative flow model of Ref. [23]). Because magnetic helicity is a nearly conserved quantity, the configurations considered here *will not* spontaneously develop poloidal magnetic fields; i.e., their helicity will remain zero. However, if a configuration were created with finite helicity (both toroidal and poloidal magnetic fields), it could relax [24] to a force-free state, whereupon vortex generation and fluid flows would cease. How much initial helicity is required for this to happen remains to be seen, but it probably involves a competition between boundary conditions trying to maintain the initial non-force-free state and internal nonaxisymmetric dynamics trying to relax to a force-free state.

Supported by NSF Grant No. ECS-8814184.

[1] Committee on Technology, *The Electric Arc Furnace-1990* (International Iron and Steel Institute, Brussels, 1990).
[2] G. R. Jones, *High Pressure Arcs in Industrial Devices* (Cambridge Univ. Press, London, 1988).
[3] R. M. Myers *et al.*, in Proceedings of the AIAA/NASA/OAI Conference on Advanced SEI Technologies, Cleveland, Ohio, September 1991, Report No. AIAA 91-3568.
[4] J. D. Sethian *et al.*, in *Physics of Alternative Magnetic Confinement Schemes, Varenna, 1990* (Editrice Compositori, Bologna, 1990), p. 511; M. G. Haines, *ibid.*, p. 277; D. Mosher and D. Colombant, Phys. Rev. Lett. **68**, 2600 (1992); D. L. Book *et al.*, Phys. Fluids **12**, 1982 (1976).
[5] J. Marshall, Phys. Fluids **3**, 135 (1960).
[6] G. Kirkman-Amemiya and M. A. Gundersen, Appl. Phys. Lett. **60**, 316–318 (1992).
[7] *MHD-Flows and Turbulence II*, edited by H. Branover and A. Yakhot (Israel Univ. Press, Jerusalem, 1980).
[8] R. D. Blandford, in *Quasars: IAU Symposium 119*, edited by G. Swarup and V. K. Kaphahi (Reidel, Dordrecht, Netherlands), p. 359, and especially p. 369.
[9] D. A. McDonald *et al.*, in *Black Holes: The Membrane Paradigm*, edited by K. S. Thorne, R. H. Price, and D. A. McDonald (Yale Univ. Press, New Haven, 1986), p. 53.
[10] H. Maecker, Z. Phys. **141**, 198 (1955).
[11] H. Edels, in *Proceedings of the Eleventh Conference on Phenomena in Ionized Gases* (Czech. Acad. Sci., Prague, 1973), Vol. 2, pp. 9–59.
[12] B. Bowman, J. Phys. D **5**, 1422 (1972).
[13] M. Irie and M. R. Barrault, J. Phys. D **10**, 1599 (1977).
[14] T. B. Reed, J. Appl. Phys. **31**, 2048 (1960).
[15] J. W. McKelliget and J. Szekely, J. Phys. D **16**, 1007 (1983).
[16] M. R. LaPointe, in Proceedings of the AIAA/NASA/OAI Conference on Advanced SEI Technologies, Cleveland, Ohio, September 1991, Report No. AIAA 91-2341.
[17] T. G. Cowling, Mon. Not. R. Astron. Soc. **94**, 39 (1934).
[18] W. H. Bennett, Phys. Rev. **45**, 890 (1934).
[19] G. R. Jones *et al.*, IEEE Proc. **129**, 611 (1982).
[20] H. Alfvén, *Cosmic Plasma* (Reidel, Dordrecht, Netherlands, 1981).
[21] *Beams and Jets in Astrophysics*, edited by P. A. Hughes (Cambridge Univ. Press, London, 1991).
[22] H. K. Moffatt, *Magnetic Field Generation in Electrically Conducting Fluids* (Cambridge Univ. Press, London, 1978), pp. 21 and 22.
[23] R. V. E. Lovelace *et al.*, Astrophys. J. Suppl. **62**, 1 (1986).
[24] J. B. Taylor, Rev. Mod. Phys. **58**, 741 (1986).

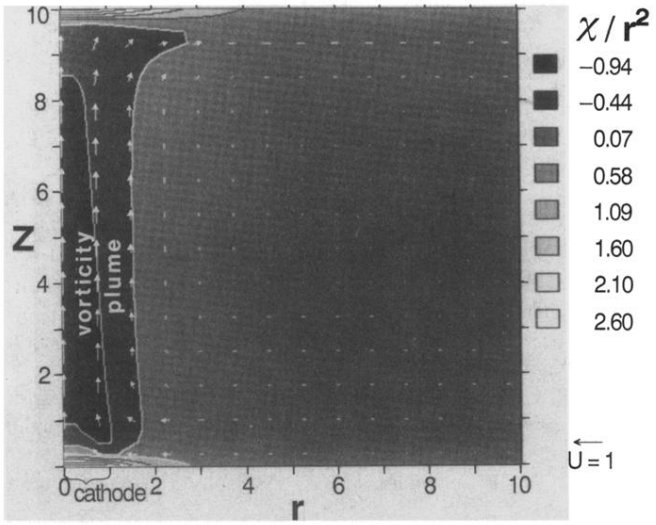

FIG. 1. χ/r^2 (shaded contours) and velocity vectors.

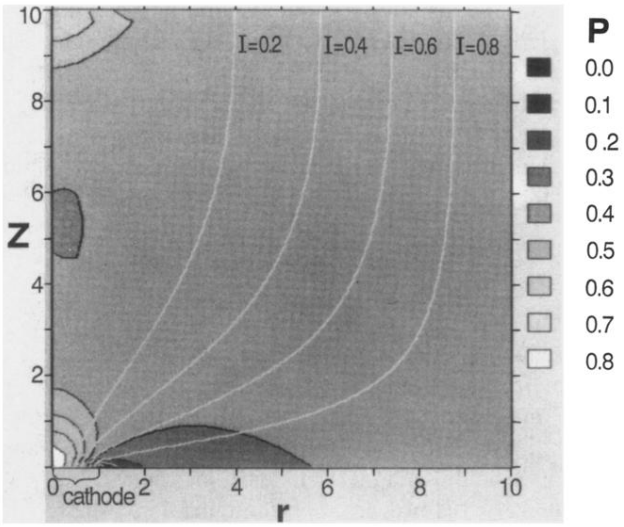

FIG. 2. P (shaded contours) and current streamlines.